

# Impedance Measurement in Frequency-Halving Networks Using a Two-Frequency Synthetic Loading Technique

ROBERT G. HARRISON, MEMBER, IEEE, AND GRIGORIOS A. KALIVAS

**Abstract** — A technique is described which removes a major difficulty in the design of wide-band frequency-halving networks: the accurate characterization of the “pumped” input and output impedances at the plane of the varactors. The procedure permits the use of realistic input and output power levels with the input at twice the output frequency.

## I. INTRODUCTION

THE optimum design of parametric frequency-halving networks employing nonlinear reactance devices such as varactors presents problems different from those encountered in the design of linear or quasi-linear networks. Although a narrow-band frequency halver has been designed using a computer technique involving an optimization strategy in the frequency domain [1], no satisfactory method has been reported for the accurate measurement of the “as pumped” large-signal input and output impedances  $Z_{in}$  and  $Z_{out}$  at the position of the varactor(s) within the halver circuit. Values for these impedances are needed in the design of matching networks in wide-band halvers.

The concept of “impedance” must be treated with some caution when designing nonlinear circuits. This is because an impedance can only be defined at a single frequency, whereas the signals associated with nonlinearities are typically rich with harmonics. Thus, use of the method given here is predicated upon the assumption that the design process has been initiated with the adoption of a halver prototype already known to operate with relatively small harmonic content at the input and output ports. The balanced halvers described in [2]–[4] can satisfy this requirement, whereas the signals associated with unbalanced halvers can have large harmonic content [1].

Thus, the method given here is not intended to bypass the need for the selection of a satisfactory starting topology. Rather, the intent is to provide a means for obtaining values for the pumped impedances  $Z_{in}$  and  $Z_{out}$  so that input and output matching networks can be designed using conventional aids such as COMPACT [5]. Attempts to optimize such networks using empirical approaches are not

usually satisfactory, particularly in the case of wide-band designs [2], [3].

In general, the pumped impedances  $Z_{in}$  and  $Z_{out}$  are quite different from the unpumped small-signal impedances and exist, for a given circuit embedding, only under appropriate and realistic conditions of input power level  $P_{in}$  and input frequency  $2\omega$ . This is because the mechanism of parametric subharmonic generation is inherently nonlinear, in the sense that there is no continuum of operational modes between linear and nonlinear regimes; indeed, since the halver is a threshold device, there is no linear regime. This is in direct contrast to a GaAs FET amplifier, for example, in which the nonlinear effects can be regarded as perturbations of what is ideally a linear process.

It follows that  $Z_{in}(2\omega)$  and  $Z_{out}(\omega)$  can only be measured in a functioning halver circuit. This dilemma can be resolved as follows.

- a) Assuming the validity of the “pumped” varactor impedance equations of Penfield and Rafuse [6], determine estimates  $\tilde{Z}_{in}(2\omega)$  and  $\tilde{Z}_{out}(\omega)$ .
- b) Use  $\tilde{Z}_{in}$  and  $\tilde{Z}_{out}$  to design a prototype halver network, e.g., with the aid of a program such as COMPACT [5].
- c) Measure the external impedances  $Z_{in}^{ext}$  and  $Z_{out}^{ext}$  of the resulting two-port.
- d) Knowing the halver network, “de-embed” the varactor impedances  $Z_{in}$  and  $Z_{out}$ , using a suitable computer procedure.
- e) Compare  $Z_{in}$  and  $Z_{out}$  with the estimates  $\tilde{Z}_{in}$  and  $\tilde{Z}_{out}$ .
- f) If the measured device impedances differ significantly from the estimates, replace the estimates by the measured values, go to b), and iterate as necessary.

Conventional load-pull techniques [7], [8] for impedance measurement in nonlinear two-ports require the determination of large-signal  $S$  parameters. For a specific input power  $P_{in}$  and input frequency  $2\omega$  the halver can be characterized by

$$\begin{bmatrix} b_1(2\omega) \\ b_2(\omega) \end{bmatrix} = \begin{bmatrix} S_{11} & S_{12} \\ S_{21} & S_{22} \end{bmatrix} \cdot \begin{bmatrix} a_1(2\omega) \\ a_2(\omega) \end{bmatrix}. \quad (1)$$

Manuscript received May 2, 1984; revised July 27, 1984. This work was supported in part by the Defence Research Establishment, Ottawa, Canada, under Contract 8SU81-0006.

The authors are with the Department of Electronics, Carleton University, Ottawa, Ontario, Canada K1S 5B6.

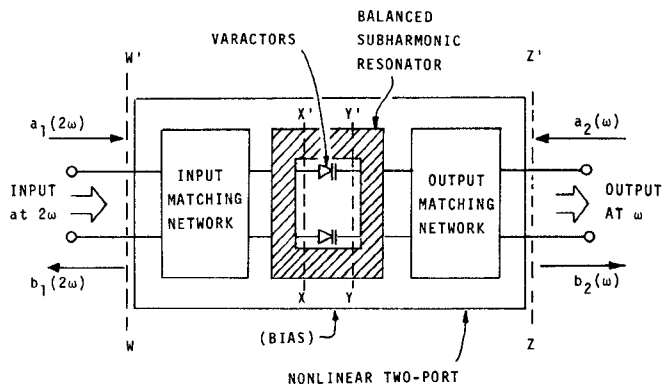


Fig. 1. Definition of two-frequency  $S$ -matrix and reference planes for balanced nonlinear frequency-halving two-port.

(See Fig. 1.) The validity of (1) depends on the supposition that only the frequencies  $2\omega$  and  $\omega$  are present at the varactor(s). It is, therefore, assumed that:

- i) The halver topology is balanced so that at the output port,  $2\omega$  and its harmonics are suppressed. Similarly, at the input port,  $\omega$  and its odd-order harmonics are suppressed.
- ii) The possible presence of varactor currents at frequencies such as  $3\omega$ ,  $5\omega$ , ... is prevented by means of suitable filters.

These conditions mean that octave-bandwidth halvers can be accommodated in the design procedure.

From (1)

$$S_{11} = \left. \frac{b_1(2\omega)}{a_1(2\omega)} \right|_{a_2(\omega) = 0} \quad (2a)$$

$$S_{12} = \left. \frac{b_1(2\omega)}{a_2(\omega)} \right|_{a_1(2\omega) = 0} \quad (2b)$$

$$S_{21} = \left. \frac{b_2(\omega)}{a_1(2\omega)} \right|_{a_2(\omega) = 0} \quad (2c)$$

$$S_{22} = \left. \frac{b_2(\omega)}{a_2(\omega)} \right|_{a_1(2\omega) = 0}. \quad (2d)$$

A network analyzer (NA) can be used to measure  $S_{11}$  at the input frequency  $2\omega$  with the output port terminated in the system characteristic impedance  $Z_0$ . The fact that the NA cannot be used to measure the transfrequency parameters  $S_{12}$  and  $S_{21}$  is of minor concern here. According to (2)–(4),  $S_{22}$  would have to be determined by applying a reverse-direction signal  $a_2(\omega)$  to the output port and measuring the resulting reflected signal  $b_2(\omega)$  from that port, the input port being terminated in  $Z_0$ , so that  $a_1(2\omega) = 0$ . An attempt to measure  $S_{22}$  in this way would result in the removal of the drive power, so that not only would halving cease, but the voltages and currents in the two-port would be completely different from those in an operating halver. This is so because, according to both theory [4] and measurement [2], [3], the frequency halver is a threshold device. That is, a suitable minimum input power  $P_{in}$  has to be established for operation in the halving mode. A similar problem was encountered by Mazumder [10], [11] in the

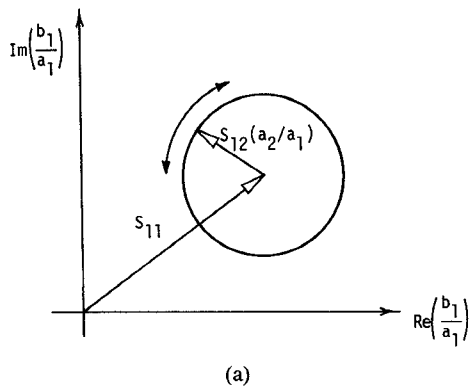


Fig. 2. Circular loci in: (a)  $b_1/a_1$ -plane at frequency  $2\omega$ , (b)  $b_2/a_2$ -plane at frequency  $\omega$ .

case of a microwave transistor operating under class  $C$  conditions.

## II. TWO-FREQUENCY MEASUREMENT TECHNIQUE

A solution is to use a two-frequency variant of the two-signal synthetic loading technique described by Takayama [9] and independently by Mazumder [10], [11]. The procedure involves the simultaneous application of the power waves  $a_1(2\omega)$  and  $a_2(\omega)$  to the input and output ports, respectively. Then no problem exists because  $|a_1(2\omega)|$  can be adjusted to obtain the required  $P_{in}$ . From (1)

$$\frac{b_1(2\omega)}{a_1(2\omega)} = S_{11} + S_{12} \frac{a_2(\omega)}{a_1(2\omega)} \quad (3a)$$

$$\frac{b_1(2\omega)}{a_2(\omega)} = S_{11} \frac{a_1(2\omega)}{a_2(\omega)} + S_{12} \quad (3b)$$

$$\frac{b_2(\omega)}{a_1(2\omega)} = S_{21} + S_{22} \frac{a_2(\omega)}{a_1(2\omega)} \quad (3c)$$

$$\frac{b_2(\omega)}{a_2(\omega)} = S_{21} \frac{a_1(2\omega)}{a_2(\omega)} + S_{22}. \quad (3d)$$

If  $|a_1|$  and  $|a_2|$  are fixed, then each of  $b_i/a_j$  ( $i=1,2$ ;  $j=1,2$ ) generates a circle in the corresponding  $b_i/a_j$ -plane (see Fig. 2) as the angle  $\angle a_1 - \angle a_2$  is varied. The center of a particular circular  $b_i/a_j$ -locus corresponds to the parameter  $S_{ij}$ .

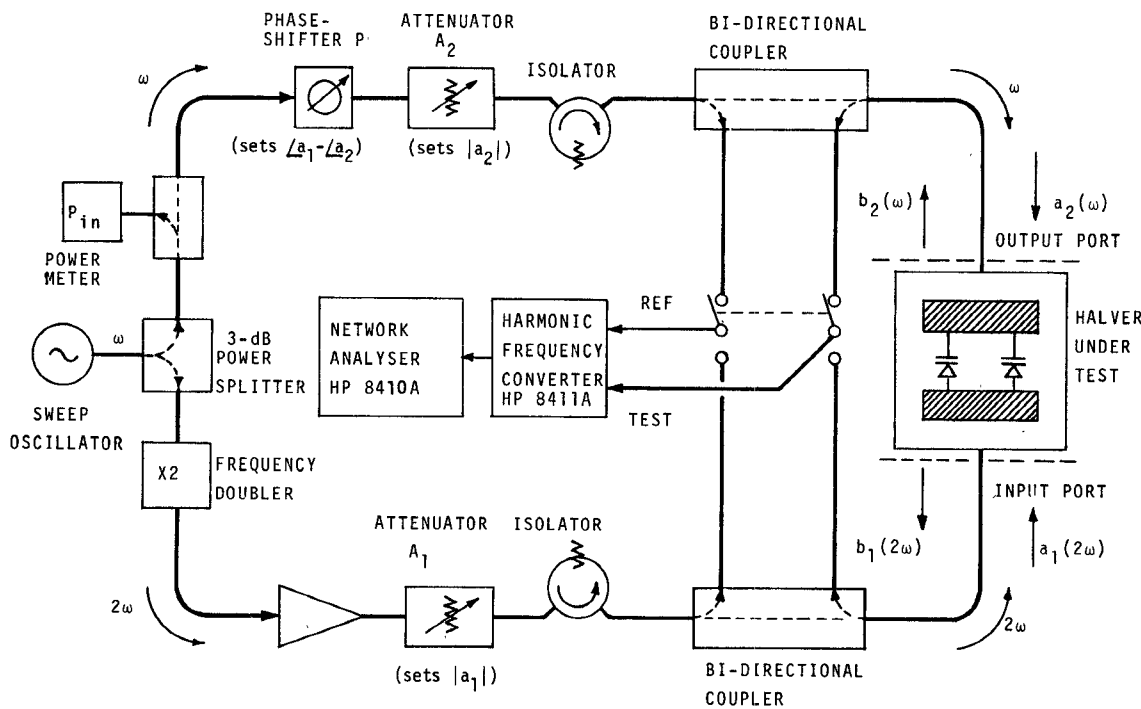


Fig. 3. Two-frequency test setup.

#### A. Basis of the Measurement Technique

The ratios  $b_1(2\omega)/a_1(2\omega)$  and  $b_2(\omega)/a_2(\omega)$  can be found from conventional NA reflection measurements by varying the angle  $\angle a_1 - \angle a_2$  using a phase shifter. This is possible because each ratio involves but a single frequency. The ratios  $b_1(2\omega)/a_2(\omega)$  and  $b_2(\omega)/a_1(2\omega)$ , on the other hand, involve two-frequency transmission measurements, which cannot be made using an NA of the normal type.

Equations (3a) and (3d) show that only  $b_1(2\omega)/a_1(2\omega)$  and  $b_2(\omega)/a_2(\omega)$  need be measured to determine  $S_{11}$  and  $S_{22}$ , respectively. The desired input and output impedances  $Z_{in}(2\omega)$  and  $Z_{out}(\omega)$  can then be obtained from  $S_{11}$  and  $S_{22}$ .

A suitable test setup is shown in Fig. 3. An important feature is the use of the synthetic load concept [9]–[11], modified here so that *different* input and output frequencies are provided for the power waves  $a_1$  and  $a_2$ . To ensure that  $a_1$  is at exactly twice the frequency of  $a_2$  and coherent with it, both signals are derived from the same sweep oscillator,  $a_2$  directly and  $a_1$  by means of a frequency doubler. Thus, as required,  $a_2$  is injected into the halver output port at exactly half the frequency at which  $a_1$  is applied to the halver input port. The phase angle  $\angle a_1 - \angle a_2$  is varied by means of the phase shifter  $P$  while the amplitudes  $|a_1|$  and  $|a_2|$  are adjusted using the variable attenuators  $A_1$  and  $A_2$ .

To obtain accurate results, a good simulation of the halving conditions is necessary. For a given input frequency  $2\omega$  and a given value of  $P_{in} = |a_1|^2$ , the power  $|a_2|^2$  injected into the output port should be such that the reflected power  $|b_2|^2$  approximates the actual  $P_{out}$  which would be obtained had the halver been terminated in a real, rather than a synthetic, load under the same conditions. This

TABLE I  
CALIBRATION MEASUREMENTS MADE AT EACH FREQUENCY AT  
BOTH PORTS OF THE HALVER UNDER TEST

CONDITION	VOLTAGE REFLECTION COEFFICIENT	
	MEASURED VALUE	TRUE VALUE
MATCHED LOAD $Z_0$	$\Gamma_{m1}$	$\Gamma_{t1} = 0$
OPEN CIRCUIT	$\Gamma_{m2}$	$\Gamma_{t2} = 1$
SHORT CIRCUIT	$\Gamma_{m3}$	$\Gamma_{t3} = -1$

value of  $P_{out}$  can be obtained from a separate measurement.

#### B. Measurement Procedure

For each input frequency, three steps are taken.

1) Calibration reflection coefficients  $\Gamma_{mj}$  ( $j=1, 2, 3$ ) are measured at the input and output reference planes  $W - W'$  and  $Z - Z'$  (as defined in Fig. 1) using a matched load, an open circuit, and a short circuit, in accordance with the scheme of Table I. Hence, complex calibration coefficients  $K$ ,  $L$ , and  $M$  are determined satisfying the bilinear transformation [12]

$$\Gamma_{mj} = \frac{K\Gamma_{tj} + L}{M\Gamma_{tj} + 1}, \quad j=1, 2, 3 \quad (4)$$

where the  $\Gamma_{tj}$  are the true values.

2) To determine the position of the circular locus in one of the complex  $b_1/a_1$ - or  $b_2/a_2$ -planes of Fig. 2, the appropriate reflection coefficient is measured, with the halver *in situ*, for three different settings of the phase

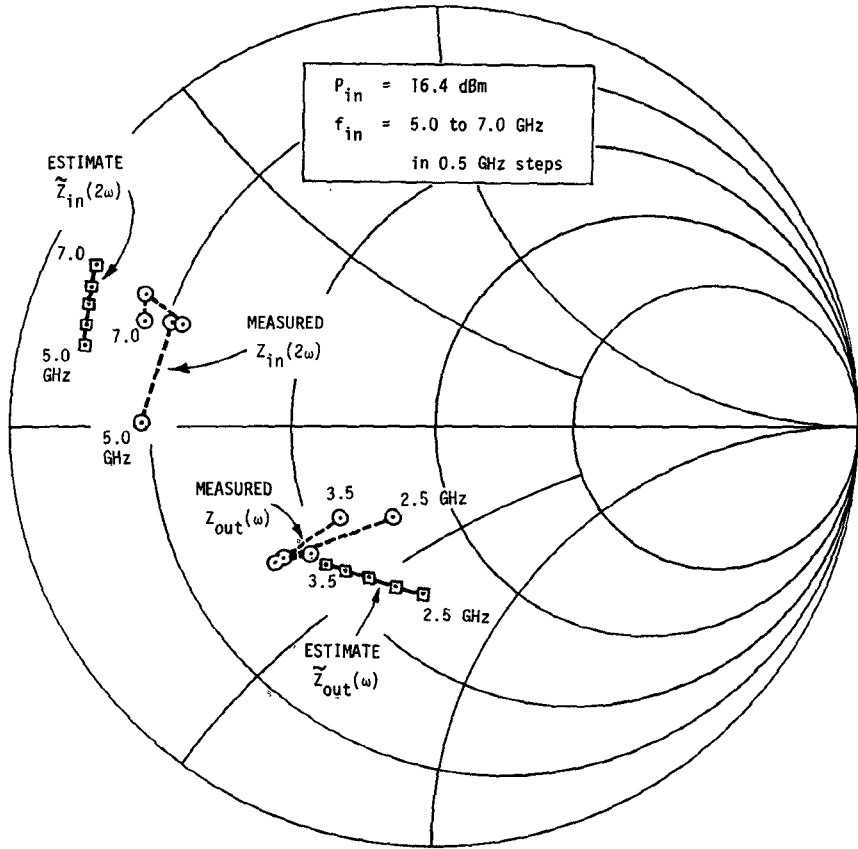


Fig. 4. Comparison between the measured input and output impedances  $Z_{in}(2\omega)$  and  $Z_{out}(\omega)$  (----) of the "pumped" varactors at the planes  $X - X'$  and  $Y - Y'$  and the estimates  $\tilde{Z}_{in}(2\omega)$  and  $\tilde{Z}_{out}(\omega)$  (—) given by (8) and (9).

shifter  $P$ , i.e., three different values of  $\angle a_1 - \angle a_2$ . This yields three measured values  $\Gamma_{mk}$  ( $k = 1, 2, 3$ ). Extraction of the true (corrected) values, which are found by solving (4)

$$\Gamma_{tk} = \frac{\Gamma_{mk} - L}{K - M\Gamma_{mk}}, \quad k = 1, 2, 3 \quad (5)$$

then locates three points on the corresponding circular locus. For the  $b_1/a_1$ - and  $b_2/a_2$ -planes the centers of the circular loci fix the values of  $S_{11}$  and  $S_{22}$ , respectively. The external impedances at the planes  $W - W'$  and  $Z - Z'$  of Fig. 1 are then

$$Z_{in}^{ext} = Z_0 \left( \frac{1 + S_{11}}{1 - S_{11}} \right) \quad (6)$$

$$Z_{out}^{ext} = Z_0 \left( \frac{1 + S_{22}}{1 - S_{22}} \right). \quad (7)$$

3) Knowing the varactor circuit environment, one can determine reflection coefficients  $\Gamma_{in}$  and  $\Gamma_{out}$  at the planes  $X - X'$  and  $Y - Y'$  of Fig. 1, e.g., by using a COMPACT de-embedding file. The required large-signal "pumped" varactor impedances  $Z_{in}$  and  $Z_{out}$  are then obtained from  $\Gamma_{in}$  and  $\Gamma_{out}$ .

### III. RESULTS

Using the procedure described above, the external impedances  $Z_{in}^{ext}$  and  $Z_{out}^{ext}$  were measured at the  $W - W'$  and  $Z - Z'$  planes of an experimental halver for  $P_{in} = 16.4$  dBm and  $|b_2|^2 - |a_2|^2 = -3$  dBm. The varactors used were

silicon tuning varactors type GC-1504, manufactured by Frequency Sources, GHZ Division. These devices have a zero-bias junction capacitance  $C_j(0) \approx 3.5$  pF and a cutoff frequency of approximately 80 GHz. The input frequency was varied over the range 5.0–7.0 GHz, the output over 2.5–3.5 GHz. Fig. 4 compares the values of  $Z_{in}$  and  $Z_{out}$  at the  $X - X'$  and  $Y - Y'$  planes, derived from the de-embedding procedure, with theoretical estimates given by the Penfield and Rafuse equations [6] modified to account for the varactor parasitics. As shown in the Appendix, for two abrupt-junction or Schottky-barrier varactors pumped in parallel at the input frequency  $2\omega$

$$\begin{aligned} \tilde{Z}_{in}(2\omega) = \frac{1}{2} \left[ r_s + \frac{m_1^2}{2m_2} \frac{\sqrt{1 + V_B/\phi}}{2\omega C_j(0)} \right] \\ + j \frac{1}{2} \left[ 2\omega L_s - m_0 \frac{\sqrt{1 + V_B/\phi}}{2\omega C_j(0)} \right] \end{aligned} \quad (8)$$

and for two varactors effectively in series at the output frequency  $\omega$

$$\begin{aligned} \tilde{Z}_{out}(\omega) = 2 \left[ m_2 \frac{\sqrt{1 + V_B/\phi}}{\omega C_j(0)} - r_s \right] \\ + j2 \left[ \omega L_s - m_0 \frac{\sqrt{1 + V_B/\phi}}{\omega C_j(0)} \right]. \end{aligned} \quad (9)$$

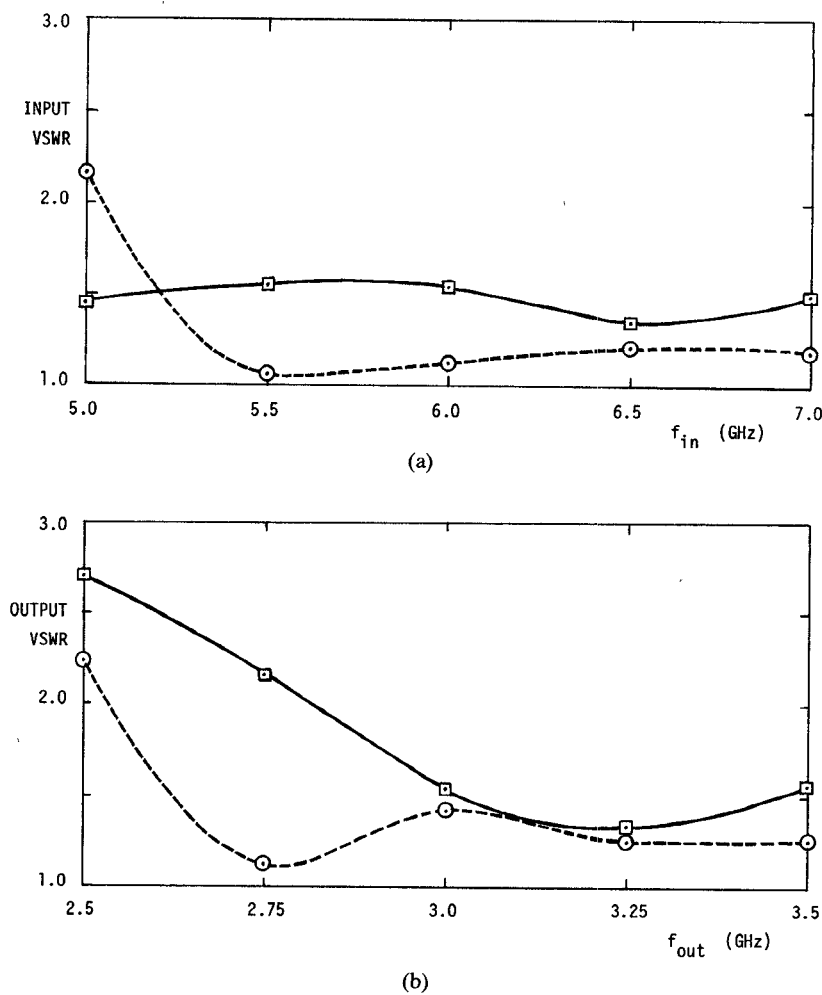


Fig. 5. Measured (----) and predicted (—) VSWR's of the frequency halver, (a) at the input plane  $W - W'$ , (b) at the output plane  $Z - Z'$ .

Here,  $C_j(0)$  is the junction depletion-layer capacitance at zero bias,  $V_B$  is the reverse breakdown voltage, and  $\phi$  is the contact potential. The varactor parasitics  $r_s$  and  $L_s$  are the series resistance and inductance, respectively.

Evaluation of (8) and (9) requires specific values for the modulation ratios  $m_0$ ,  $m_1$ , and  $m_2$ , corresponding to zero frequency and the output and input frequencies, respectively. According to [6], under full-drive maximum-efficiency conditions, the modulation ratios would be  $m_0 = 0.5$ ,  $m_1 = 0.21$ , and  $m_2 = 0.1$ . These values assume that the varactor is so biased that the junction elastance waveform is symmetrical. In practical frequency halver applications, however, the varactors are usually zero-biased or slightly forward-biased; the resulting elastance waveform is highly asymmetrical. As discussed in the Appendix, under such conditions, more appropriate values for the modulation ratios would be approximately  $m_0 = 0.2$ ,  $m_1 = 0.2$ ,  $m_2 = 0.15$ . These were the values adopted in the present example.

It is seen that there is satisfactory agreement between the measured varactor impedances  $Z_{in}(2\omega)$ ,  $Z_{out}(\omega)$  and the estimates  $\tilde{Z}_{in}(2\omega)$ ,  $\tilde{Z}_{out}(\omega)$ , and that in this case a single iteration suffices.

Fig. 5 compares the measured and predicted VSWR's at the external ports of the complete halver. Again, there is reasonable agreement between the measured and calculated VSWR's.

#### IV. CONCLUSIONS

It has been demonstrated that a two-frequency variant of the synthetic loading technique provides an effective approach to the determination of the "pumped" input and output impedances of the internal nonlinear-reactance device(s) of a frequency halver. These are the impedances which are needed for design centering.

A similar approach could be used in the design of frequency doublers; in that case a halver would replace the doubler in the test setup.

#### APPENDIX THEORETICAL ESTIMATE OF VARACTOR IMPEDANCES

For the balanced halvers of the type investigated here, the two varactors are effectively in parallel for the input frequency  $2\omega$  but in series for the output frequency  $\omega$ .

An approach similar to that of Penfield and Rafuse [6] can be used to obtain the estimates  $\tilde{Z}_{in}(2\omega)$  and  $\tilde{Z}_{out}(\omega)$

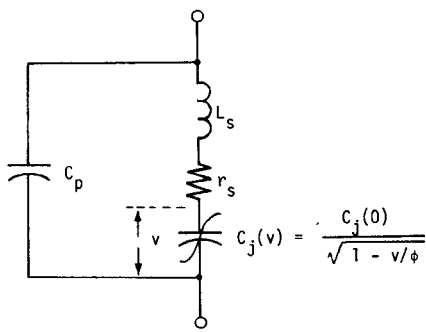


Fig. 6. Approximate equivalent circuit of a single unpumped varactor.

for the drive-level-dependent "as pumped" input and output impedances of the varactor pair. The approximate equivalent circuit of Fig. 6 is assumed for a single unpumped varactor. Since the package capacitances  $C_p$  can be absorbed into the embedding, they can be omitted from this discussion. As in [6], in order to obtain closed-form expressions, this large-signal analysis is restricted to abrupt-junction or Schottky-barrier devices, for which the capacitance-law exponent  $\gamma$  is approximately  $1/2$ . For varactors with other values of  $\gamma$ , the impedance estimates will be less accurate, but will still provide useful starting values.

#### Output Impedance

Consider first a single pumped varactor in which currents are constrained to flow only at  $\omega$  and  $2\omega$ . Assuming a load  $Z_L$  at the output-frequency port and initially neglecting the series inductance  $L_s$ , the following relationship is found between  $Z_L$  and the drive-level dependent elastance coefficients  $S_0$  and  $S_2$  of the varactor:

$$\left| Z_L + r_s + \frac{S_0}{j\omega} \right| = \frac{|S_2|}{\omega}. \quad (10)$$

Here, the  $S_k$  are complex coefficients of the Fourier expansion of the time-varying incremental varactor elastance

$$S(t) = \sum_{k=-\infty}^{+\infty} S_k e^{jk\omega t}. \quad (11)$$

By definition, the *large-signal* cutoff frequency of the varactor is

$$\omega_c \triangleq \frac{S_{\max} - S_{\min}}{r_s} \quad (12)$$

where  $S_{\max}$  and  $S_{\min}$  are the extreme elastance values to which the device is pumped. Further, modulation ratios are defined as

$$m_k \triangleq \frac{|S_k|}{S_{\max} - S_{\min}}. \quad (13)$$

The following relation between the  $m_k$  and the  $S_k$  is then obtained from (12) and (13):

$$|S_k| = m_k \omega_c r_s. \quad (14)$$

From (10) and (14), the resistive and reactive components

of  $Z_L$  are found to be

$$R_L = r_s \left( m_2 \frac{\omega_c}{\omega} \cos \theta - 1 \right) \quad (15)$$

and since  $S_0 = |S_0|$

$$X_L = r_s \frac{\omega_c}{\omega} (m_2 \sin \theta + m_0) \quad (16)$$

where  $\theta$  is the phase angle of the impedance  $Z_L + r_s + S_0/(j\omega)$ . For fixed values of  $m_k$  and  $\omega$ , the maximum efficiency condition is  $\theta = 0$ . Assuming that this results in a conjugately matched load, the effective varactor output impedance seen looking back from the load terminals is, since  $|S_0| = S_0$

$$Z_L^* = r_s \left( m_2 \frac{\omega_c}{\omega} - 1 \right) - j m_0 \frac{\omega_c}{\omega} r_s. \quad (17)$$

To evaluate  $\omega_c$ , full drive is assumed, so that

$$S_{\max} = \frac{1}{C_j(-V_B)} \quad (18)$$

and

$$S_{\min} = \frac{1}{C_j(\phi)} \approx 0 \quad (19)$$

where  $V_B$  and  $\phi$  are, respectively, the reverse breakdown and contact potentials of the varactor. Taking the capacitance law for  $\gamma = 1/2$  as

$$C_j(v) = C_j(0) \left( 1 - \frac{v}{\phi} \right)^{-1/2} \quad (20)$$

where  $v$  is the junction voltage, the large-signal cutoff frequency is, in terms of easily measured parameters

$$\omega_c = \frac{\sqrt{1 + V_B/\phi}}{r_s C_j(0)}. \quad (21)$$

Thus, for two varactors effectively in series at the output frequency, an estimate of the pumped output impedance is, from (17) and (21), and including  $L_s$ ,

$$\begin{aligned} \tilde{Z}_{\text{out}}(\omega) = 2 & \left[ m_2 \frac{\sqrt{1 + V_B/\phi}}{\omega C_j(0)} - r_s \right] \\ & + j 2 \left[ \omega L_s - m_0 \frac{\sqrt{1 + V_B/\phi}}{\omega C_j(0)} \right]. \end{aligned} \quad (22)$$

#### Input Impedance

From [6], the pumped input impedance  $Z_{\text{in}}$  of a single varactor, at the frequency  $2\omega$ , again neglecting  $L_s$  and  $C_p$ , has resistive and reactive components

$$R_{\text{in}} = r_s \left( 1 + \frac{m_1^2}{2m_2} \cdot \frac{\omega_c}{2\omega} \cos \theta \right) \quad (23)$$

$$X_{\text{in}} = -r_s \frac{\omega_c}{2\omega} \left( m_0 + \frac{m_1^2}{2m_2} \sin \theta \right). \quad (24)$$

Setting  $\theta = 0$ , as before

$$Z_{\text{in}} = r_s \left( 1 + \frac{m_1^2}{2m_2} \cdot \frac{\omega_c}{2\omega} \right) - j r_s \frac{\omega_c}{2\omega} m_0. \quad (25)$$

Therefore, for two varactors in parallel at the input frequency, an estimate of the input impedance is, using (21) and (25), and including  $L_s$ ,

$$\begin{aligned} \tilde{Z}_{in}(2\omega) = & \frac{1}{2} \left[ r_s + \frac{m_1^2}{2m_2} \cdot \frac{\sqrt{1+V_B/\phi}}{2\omega C_j(0)} \right] \\ & + j \frac{1}{2} \left[ 2\omega L_s - m_0 \cdot \frac{\sqrt{1+V_B/\phi}}{2\omega C_j(0)} \right]. \quad (26) \end{aligned}$$

### Estimates for the Modulation Ratios

Application of (8) and (9) for the approximate device impedances requires estimates for the modulation ratios  $m_0$ ,  $m_1$ , and  $m_2$ . In [6, p. 469], Penfield and Rafuse give an idealized optimum-efficiency solution for an abrupt-junction varactor fully driven between the forward contact potential  $\phi$  and the reverse breakdown voltage  $V_B$ . This solution requires a reverse-bias voltage of approximately  $0.35V_B$  and predicts a *symmetrical* elastance waveform  $S(t)$  for which the modulation ratios are  $m_0 = 0.5$ ,  $m_1 = 0.21$ , and  $m_2 = 0.08$ .

Under conditions of zero bias, or small forward bias, which are applicable to practical wide-band halvers, these values for the modulation ratios are inappropriate. This can be deduced from the example of the zero-biased single-varactor voltage waveform  $v(t)$  obtained by Lipparini *et al.* [1, fig. 6] for a partially driven unbalanced halver with an input frequency of 2.375 GHz. The corresponding  $S(t)$  waveform can be found by means of the parabolic elastance-voltage relationship for an abrupt junction

$$S(v) = \frac{1}{C_j(0)} \sqrt{1 - v/\phi} \quad (27)$$

and is found to be highly *asymmetrical*. The resulting modulation ratios for a fully-driven case are thus estimated to be  $m_0 \approx 0.2$ ,  $m_1 \approx 0.2$ , and  $m_2 \approx 0.15$ .

### ACKNOWLEDGMENT

The authors wish to thank Dr. W. D. Cornish for his encouragement. The constructive suggestions of two anonymous reviewers are gratefully acknowledged.

### REFERENCES

- [1] A. Lipparini, E. Marazzi, and V. Rizzoli, "A new approach to the computer-aided design of nonlinear networks and its application to microwave parametric frequency dividers," *IEEE Trans. Microwave Theory Tech.*, vol. MTT-30, pp. 1050-1058, July 1982.
- [2] R. G. Harrison, "A broad-band frequency divider using microwave varactors," *IEEE Trans. Microwave Theory Tech.*, vol. MTT-25, pp. 1055-1059, Dec. 1977.
- [3] —, "A broad-band frequency divider in waveguide," in *1978 IEEE MTT-S Int. Microwave Symp. Dig.*, (Ottawa, Canada), June 1978, pp. 257-259.
- [4] —, "Theory of the varactor frequency halver," in *1983 IEEE MTT-S Int. Microwave Symp. Dig.*, (Boston, MA), June 1983, pp. 203-205.

- [5] "COMPACT User's Manual," Comsat General Integrated Systems, Palo Alto, CA, 1979.
- [6] P. Penfield and R. P. Rafuse, *Varactor Applications*. Cambridge, MA: M.I.T. Press, 1962, pp. 454-473.
- [7] W. H. Leighton, R. J. Chaffin, and J. G. Webb, "RF amplifier design with large-signal S-parameters," *IEEE Trans. Microwave Theory Tech.*, vol. MTT-21, pp. 809-814, Dec. 1973.
- [8] O. Müller, "Large-signal S-parameter measurements of class C operated transistors," *Nachrichtentech. Z.*, vol. 21, no. 10, pp. 644-647, Oct. 1968.
- [9] Y. Takayama, "A new load-pull characterization method for microwave power transistors," in *1976 IEEE MTT-S Int. Microwave Symp. Dig.*, (Cherry Hill, NJ), June 1976, pp. 218-220.
- [10] S. R. Mazumder, "Characterization and design of microwave class C transistor power amplifiers," Department of Electronics, Carleton University, Ottawa, Canada, Ph.D. dissertation, Nov. 1976.
- [11] S. R. Mazumder and P. D. van der Puije, "Two-signal method of measuring the large-signal S parameters of transistors," *IEEE Trans. Microwave Theory Tech.*, vol. MTT-26, pp. 417-420, June 1978.
- [12] B. A. Syrett, "Computer-aided large-signal measurement of IMPATT-diode electronic admittance," *IEEE Trans. Microwave Theory Tech.*, vol. MTT-27, pp. 830-834, Oct. 1979.



Robert G. Harrison (M'82) was born in London, England, on July 29, 1932. He received the B.A. and M.A. (Eng.) degrees from Cambridge University, London, England, in 1956 and 1960, respectively, and the Ph.D. and D.I.C. from the University of London, London, England, in 1964.

From 1964 to 1976, he was with the Research Laboratories of RCA Ltd., Ste-Anne-de-Bellevue, Quebec, Canada, where he carried out research on nonlinear microwave devices. In 1977, he became Director of Research at Com Dev Ltd., Dorval, Quebec, where he worked on microwave frequency-division networks. From 1979 to 1980, he was a Communications Systems Specialist at Canadian Marconi Company, Montreal, Quebec, working on spread-spectrum systems. Since 1980, he has been Professor of Engineering in the Department of Electronics, Carleton University, Ottawa. His current research interests include spread-spectrum frequency synthesizers, the exploitation of nonlinear effects in microwave semiconductor devices, and linearization techniques for satellite transponders. He holds a number of basic patents in the area of microwave frequency-division devices and received the "Inventor" award from Canadian Patents and Development in 1978.



Grigorios A. Kalivas was born in Trikala, Greece, on January 1, 1958. He received the Diploma in Electrical Engineering from the University of Patras in 1980 and the M.Eng. degree from Carleton University, Ottawa, Ontario, Canada, in 1982. Since 1980, he has been a Research Assistant at the Department of Electronics, Carleton University, where he is currently working on his Ph.D. program.

His research interests include microwave theory and device design as well as spread-spectrum communications with emphasis on frequency synthesizers used in frequency-hopping systems.

Mr. Kalivas is a member of the National Technical Chamber of Greece.